*Biomechanics and Modeling in Mechanobiology*

# Implementation of a specific boundary condition for a simplified symmetric single path CFD lung model with OpenFOAM

A. Pandal-Blanco[1], R. Barrio-Perotti[1], R. Agujetas-Ortiz[2], A. Fernández-Tena[3]

[1]Departamento de Energía, Universidad de Oviedo, Spain

[2]Departamento de IMEM, Universidad de Extremadura, Spain

[3] Instituto Nacional de Silicosis, Spain

**Abstract**

CFD modelling research about the lung airflow with a complete resolution and an adequate accuracy at all scales requires a great amount of computational resources due to the vast number of necessary grid elements. As a result, a common practice is to conduct simplifications that allows to manage it with ordinary computational power. In this study, the implementation of a special boundary condition in order to develop a simplified single conductive lung airway model, which exactly represents the effect of the removed airways, is presented. The boundary condition is programmed in the open-source software OpenFOAM® and the developed source code is presented in the proper syntax. After this description, modelling accuracy is evaluated under different flow rate conditions typical of human breathing processes, including both inspiration and expiration movements. Afterwards, a validation process is conducted using results of a Weibel's model (0-4 generations) simulation for a medium flow rate of 50 L/min. Finally, a comparison against the proposed boundary condition implemented in the commercial code ANSYS Fluent is made, which highlights the benefits of using the free code toolbox. The specific contribution of this paper will be to show that OpenFOAM® developed model can perform even better than other commercial codes due to a precise implementation and coupling of the default solver with the in-house functions by virtue of the open-source nature of the code.

Keywords: boundary condition, CFD, human airways, OpenFOAM®, single airway, truncated branches

## INTRODUCTION.

Computational fluid dynamics or CFD is the technique used by computers to simulate the movement of fluids by solving the differential equations in partial derivatives that govern their movement and determining the boundary conditions of the different domains studied. For this reason, training in fluid mechanics and knowledge of the philosophy, capabilities and limitations of the system have become very important for CFD management so that the results obtained are correct and useful. Nowadays CFD is a basic tool for the design and development of racing cars, aerospace vehicles and wind turbines because they are the

usual field of work of mechanical engineers. However, there is also another important research field for engineers in the human body, where fluids play an important role, due to blood moves through the vessels and air flows into the lungs. Therefore, the collaborative work between engineers and physicians has led to a field called bioengineering. The physicians provide the description of the organs and their operation and the engineers build the model and simulate its performance.

Regarding lung research, it is first needed to know its geometry to be able to build a model. The human respiratory system can be divided into two parts: upper airway, consisting of the nostrils, mouth, pharynx, larynx, and lower airway (lung), consisting of conductive zone (trachea, bronchi) and respiratory zone (alveolar ducts and sacs), being the cricoid cartilage, located in the larynx, the point of separation between the two parts. Next step is to build the model. The first mathematic model for particle deposition was done in 1935 by Findeisen[11]. This author divided the respiratory tract into only 9 generations, reaching alveolar ducts and sacs. Other authors used and improved Findeisen's model (Landhal[23], Beekmans[6], Davies[7]) although the most commonly used anatomical model was developed by Weibel[32] in 1963. In this model, the ways of bifurcation are indicated, designating the trachea as the first airway (order 0) and presuming that each airway leads to two branches (regular dichotomy). Weibel described a minimum of 23 airway generations up to the alveolar ducts. On the contrary, detailed mathematical descriptions were proposed by Sauret et al.[26], Hegedus et al.[14] and Schmidt et al.[28], providing high-resolution models of morphologically realistic airways up to the fifth generation. In this line, algorithmic techniques were also proposed by Kitaoka et al.[21] and Tawhai and Burrowes[29] in order to describe the geometry of the lower airways. In any case, considering the basic morphology of Weibel[32], it can be deduced that the number of individual airway segments for the entire lung is more than 16 million. Then, a computational resolution of the complete flow at all scales with an adequate accuracy would require a mesh size of the order of several billions of elements, making it impossible to simulate, so it becomes necessary to simplify it.

A first approach to this problem is to work on several series of small airways sections (Nowak et al.[24], Zhang et al.[36]), with the great issue of prescribing the output boundary condition at the end of each section before running the calculations of the next one. Another works directly studied isolated sections of the lung (Adler[1], Ball[4,5], Grosse[13], Theunissen[30], Yang[34,35], Zhang[37]). Although these studies represented a significant advance for the simulation of airflow in the lungs, this sequential procedure does not allow a full flow coupling at all scales. Another trend to solve this problem is to use truncated lungs, cutting some branches and putting appropriate boundary conditions at these terminations. The definition of the correct boundary condition is the major point, for example Gemci et al.[12] imposed on the unresolved regions a constant pressure but the results showed that the pressure drop through all the predicted geometry was 30% less than the value obtained in the experimental study of Hyatt and Wilcon[15]. Fernández-Tena et al.[9,10] simulate the entire

conductive area of the lung using a single path symmetrical model, in which the flow conditions (velocity vector at each cell) of a cross section of the conductive branch are copied in their symmetric of the truncated branch, following the idea used by Walters[31] and Koullapis[22], with the advantage of making an exact copy of the existing velocity profile which allows a perfect flow simulation, both in inhalation and exhalation processes. Moving a step forward the simplification, recent works of Kannan et al. [16,17,18,19,20] adopt the Quasi-3D format instead of a full CFD showing promising results with a huge computational cost reduction, being possible to handle truncated lung models and also particle deposition.

However, research work should be directed towards patient specific treatment and thus, real characteristics should be retained. It is proposed to obtain a real lung geometry from a CT scan (till around 3 to 5 generations) and then, coupled the STL geometry with a symmetric single path ideal model with the same type of function presented in Fernández-Tena et al.[9], which places the velocity field of a cross section of the conductive path in its symmetric of the truncated path. The objective of this paper is to develop the tools able to perform accurate lung airflow simulations by means of free open-source software OpenFOAM®[33] and to demonstrate that it can perform the same tasks as other payment programs showing an even better performance.

## MATERIALS AND METHODS.

### Geometry Creation

The construction of the three-dimensional airway model has been made following the proposed one by Kitaoka et al.[21] supplemented with Weibel's model[32]. The classic model of Weibel indicates the bifurcation modes, designing the trachea as the first airway (order 0) and assuming that each airway generates two new branches (regular dichotomy). So, the left and right main bronchi are order 1 and so on, and there are 23 airway generations until the alveolar sacs. According to this model, there is 1 order 0 ($2^0$), 2 airways of order 1 ($2^1$), 4 airways of order 2 ($2^2$) and 8,388,608 airways of order 23($2^{23}$). In Weibel's model[32] wasn't taken into account the spatial disposition of the branches,being considered a planar layout. Kitaoka et al.[21] achieved the design of a realistic three-dimensional model of the lung, elaborated through nine basic rules: branching is dichotomous; the parent branch and its two daughter branches lie in the same plane; the volumetric flow rate through the parent branch is conserved after branching; the region supplied by a parent branch is divided into two daughter regions by a plane called the space-dividing plane perpendicular to the branching plane; the flow-dividing ratio is set to be equal to the volume-dividing ratio, defined as the ratio of the volume of the smaller daughter region to that of its parent; diameters and branching angles of the two daughter branches are determined by algebraic equations; the length of each daughter branch is set to three times its diameter; if branching continues in a given direction, the daughter branch becomes the new parent branch, and the associated branching plane is set perpendicular to the branching plane of

the old parent while the angle between the two successive branching planes is called the rotation angle of the branching plane; the branching process in a given direction stops whenever the flow rate becomes less than a specified threshold or the branch extends beyond its own region. These recommendations were followed for the development of the model up to the conductive airway (16$^{th}$ generation). More details of how the model has been built can be seen in Fernández-Tena[8], being developed using the commercial geometry and grid generation software Ansys Gambit®[3].

A reduced model of the single-path lung has been made from the complete symmetrical model shown in Figure 1, truncating one of the daughter branches downstream of each bifurcation. It is evident that this model requires a significantly lower computational cost in relation to a complete airway model (at the end of 16$^{th}$ generation there are 65,536 paths).

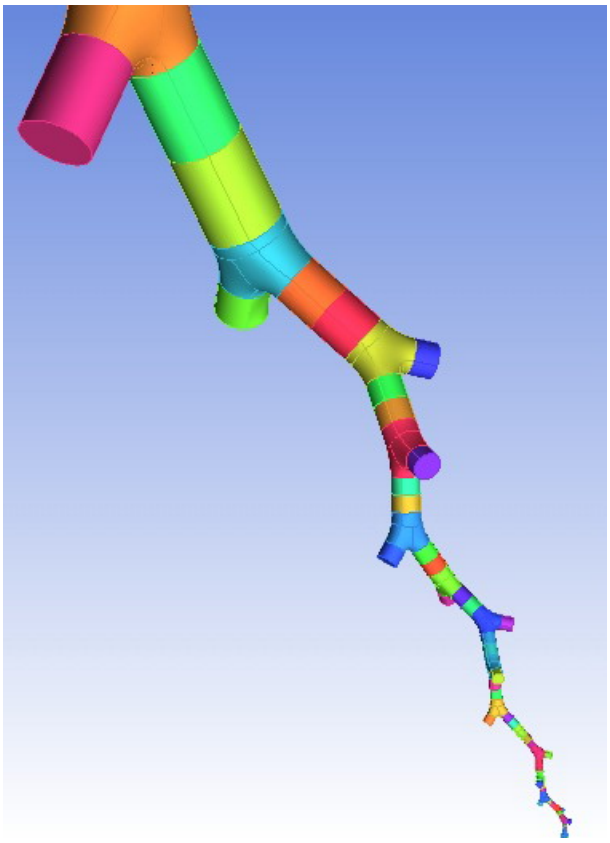

*Figure 1. Geometry of the numerical reduced model of the single-path lung*

The mesh of the model was built using an external boundary layer mesh composed of triangular prisms and a tetrahedral mesh in the interior, in such a way that the size of the mesh decreased as they descended from high-order to low-order generations, so as to maintain the same relative size throughout (i.e., the size of the mesh with respect to the diameter of the mesh). The prisms were extruded in the domain of the triangular mesh in the wall of the airway, and the unstructured tetrahedral mesh were used to fill the rest of the volume, with a total number of cells of approximately one million. A mesh quality analysis showed a very satisfactory result, indicating a magnitude of the equisized skew

below of 0.6 for 98% of the cells. Figure 2 shows an example of the surface mesh for some airway segments as well as a display of the prismatic boundary layer mesh together with a description of the parameters used to generate it. The boundary layer is comprised of 6 rows of 32 cells along the diameter of each airway segment applying a grow factor of 20% between rows. For the first cell, closest to the wall, the height is defined as the 10% of its width. With this construction and thanks to the small velocities and densities to be tested a y+ value lower than 5 is easily achieved (mean value 2.37). Additionally, a grid dependence analysis was carried out before performing the final calculations. For this purpose, two additional finer grids of size $2 \cdot 10^6$ and $4 \cdot 10^6$ cells were built in order to check the change in the magnitude of two reference variables as a function of the number of cells. The reference variables chosen were the static pressure and the volumetric flow rate at the lowest generation. It was observed that the typical variations predicted with the baseline mesh were below 1.5% (when compared to the results of the finest grid). At the end, taking into account the computational effort, the baseline grid ($10^6$ cells) was selected to conduct the different studies. Additionally, a pure Weibel's model for 0-4 generations has been constructed in order to validate the performance of the proposed boundary condition for a single lung path.

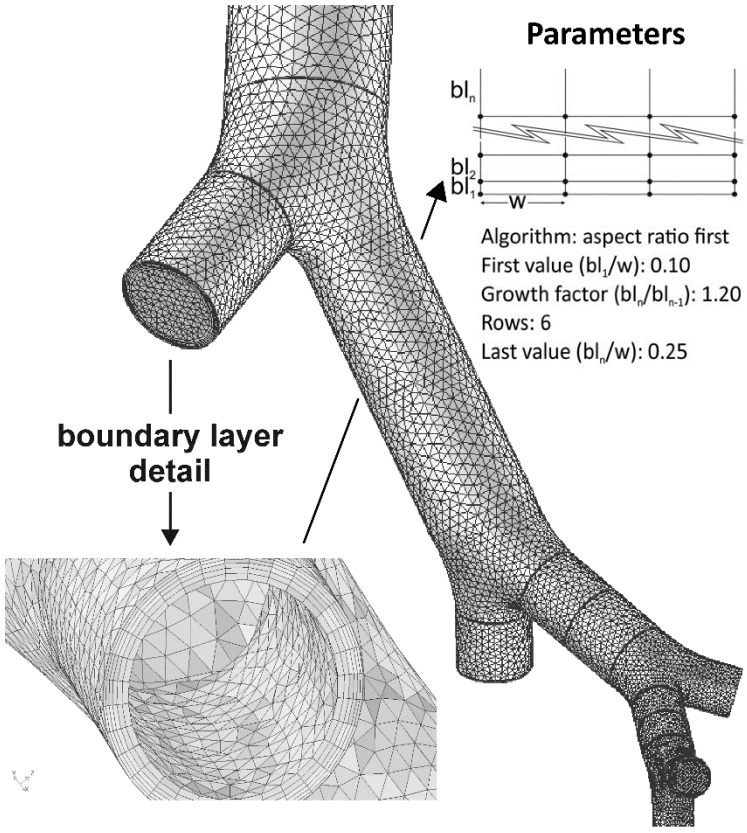


*Figure 2. Surface meshes at some branches and a detail of the boundary layer mesh in a truncated airway segment*

Boundary Condition Implementation

As well explained in Fernández-Tena et al.[9], the truncated branches in the airways require a special boundary condition which must represent precisely the effect of the removed airways. In the present study, a new OpenFOAM®[25,33] boundary condition has been developed following the work of Fernández-Tena et al.[9]. Then, making use of the symmetrical characteristics of the lung model, every truncated branch (where the boundary condition should be applied) could be paired with its symmetrical surface, associated interior face (intassoc), within the conductive branch. As a result, the velocity vector of each of the mesh faces of the associated interior face could be copied to the corresponding mesh faces in its symmetrical truncated branch (bc).

Therefore, it needs an identifier list which can relate every face of the selected bc with the symmetrical one in the conductive branch. With the aim of creating an efficient solver, this phase of the numerical model is conducted outside of the SIMPLE loop algorithm at the beginning of the calculation, then it is only made one time due to it is going to be constant. This process starts by the creation of a mirror image of the interior face, which is a *faceZone* in OpenFOAM® nomenclature, with respect to a plane that includes its geometrical center and is parallel to the symmetry plane of the bifurcation. The (geometrical) centers of these faces are obtained by means of the center of mass, which is equal to the sum of the products of the center of each cell *(faceI)* and its area divided by the face area. This is made inside of a loop for all the existing *faceZones (fZone)* of the model, in this case, 16 is considered as the number of generations in the model.

```
forAll (fZone, faceI)
{
    center[faceI]=mesh.Cf()[fZone[faceI]];
    area[faceI]=mesh.magSf()[fZone[faceI]];
    faceA += area[faceI];
}
fzOrigen = gSum(center * area) / faceA
```

Afterwards, a similar procedure is followed to obtain the centers of the faces within each bc (truncated branches). Then, a translation equal to the centers distance is applied to the mirror image and at the end of this operation both surfaces are overlapped (see Figure 3).

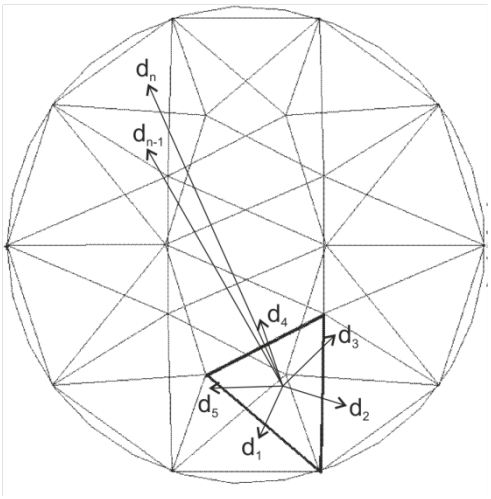


*Figure 3. Truncated and interior face overlapped. Minimum distance between mesh faces is calculated to find associated pairs*

Subsequently, the faces of these superposed surfaces should be related in order to feed with the proper information the boundary condition. As presented in Fernández-Tena et al.[9] the distances of the centers of every mesh face of the truncated boundary (bc) is compared with all mesh faces of the translated interior face(intasoc). The mesh face pair whose distance between centers is a minimum is associated together and thus, its corresponding index are kept in a relations list. The key at this step is to create the list with the necessary characteristics to be accessible from a boundary condition file. This is solved by means of an *IOList* in OpenFOAM® syntax. At the end of this phase, a complete set of associated pairs of mesh faces is obtained and stored.

The final step consists of applying an algorithm that assures the same velocity profile in the boundary condition (truncated face) and its symmetrical face within the continuous path (intasoc), once the solution is converged at each time step. Due to the presence of different truncated faces in the lung model, the first goal is to identify from the list of existing bc the index of the one which is going to be calculated:

```
scalar indexBC (-1);
forAll (bcNames, i)
{
        if (bcNames[i].compare(patch().name()) == 0) {indexBC = i;}
}
if (indexBC == -1){FatalError<< "Boundary condition name not found!" << exit(FatalError);}
```

Then, to have access to the velocity field of the proper intasoc (faceZone) a nested process is followed, starting from the general mesh and going deeper till the cells in contact with the intasoc surface.

```
//Load U field to access values on the mesh
constvolVectorField& U = this->db().objectRegistry::lookupObject<volVectorField> ("U");
//Load the mesh in order to access the faceZones
```

```
constfvMesh& mesh = U.mesh();
//Identify the desired internal faceZone
label zoneID = mesh.faceZones().findZoneID(faceZoneNames[indexBC]);
// check face has been found
if(zoneID == -1){FatalError<< "face not found!" << exit(FatalError);}
//Load the mesh of the desired internal faceZone
constfaceZone&fZone = mesh.faceZones()[zoneID];
constlabelList&masterCells = fZone.masterCells(); //cells on one side of the faceZone;
constlabelList&slaveCells = fZone.slaveCells(); //cells on the other side of the faceZone;
```

Finally, a loop over the cells within the boundary condition (truncated branch) is made in order to set its velocity equal to the one of the corresponding cell at the intasoc. However, a stiff relation conducts to stability issues and as a result, a relaxation method is implemented. Thus, the new velocity at the bc is equal to the one in the previous iteration plus the difference between the actual velocities of the bc cells and the ones from the intasoc, multiplied by an under-relaxation coefficient:

$$bcVel_i = bcVel_{i-1} + C_{RELAX} \cdot (inVel_i - bcVel_{i-1})$$

where $bcVel_i$ is the value of velocity to be applied in the truncated face (bc) at iteration i, $bcVel_{i-1}$ is the value of velocity in the truncated face (bc) at iteration i − 1, $inVel_i$ is the value of velocity in the symmetric face (intasoc) at iteration i, and $C_{RELAX}$ is the value of the under-relaxation coefficient.

For the current study, an under-relaxation coefficient of 0.5 was used. It is apparent that this procedure will force the bc face velocities to relax to their corresponding intasoc face values as the simulation converges over several iterations.

CFD Model Set-Up

Two different CFD codes are used in this study. On the one hand, the commercial code Ansys FLUENT®[2] in which the boundary condition is implemented trough an User Defined Function (UDF), as in Fernandez-Tena et al. [9,10] works; and on the other the free software OpenFOAM® for which the implementation is described in the present work. Both CFD codes are used to solve the steady Reynolds-averaged Navier-Stokes equations by means of pressure-based implicit formulations that use the SIMPLE algorithm to solve the coupling between pressure and velocity fields. Turbulent closure was accomplished with the SST k-ω model with default constant values and enhanced wall treatment to solve the flow field close to the walls. Air was the working fluid with a constant density of 1.225 kg/m3 and dynamic viscosity of 1.7894 × 10−5 kg/(m s).

The boundary conditions imposed were a constant flow rate at the inlet and a constant and uniform static pressure at the terminal outlet, while the new developed boundary condition is used at each of the truncated branches. In order to assure the robustness and reliability of the new model, several steady simulations were run within the range of 10 to 90 L/min,

considering both inspiration and exhalation cases. They were run to full convergence, which was measured by a reduction in all flow residuals by at least 4 orders of magnitude, as well as a relative change in measured parameters (pressure and flow rates in selected airways) less than $10^{-5}$ from one iteration to the next, indicating that a steady state condition had been achieved. Regarding numerical schemes, the discretization of the divergence terms was solved with a second order scheme, and a first order Euler scheme is applied for time derivative terms.

**RESULTS.**

Boundary Condition Validation

First of all, it is desired to verify the accuracy of the implemented boundary condition by means of the comparison between mean values calculated at the truncated faces (bc) and the values on the corresponding interior faces (intasoc), for both velocity and pressure. The values of velocity correspond to the average velocity of each face while pressure values represent pressure difference between each face and the inlet pressure. Note that pressure loss values are represented as absolute values for a better comparison between the inspiration and expiration conditions. In Figure 4 to 6 velocities (blue lines) and pressure losses (red lines) are compared for each pair of faces at the same level during inspiration or expiration cases, regarding the different flow rates evaluated.

Overall, it can be noted the great performance shown by the model. For both quantities the profiles calculated at the bc match perfectly the ones shown at the intasoc. In this regards, in Table 1 the mean relative error has been collected for each flow rate condition. At lowest flow rate, the error in terms of pressure losses is quite low while the velocity one is around a 1%. Increasing the flow rate leads to better accordance in terms of velocity and a slightly worse results for pressure losses. In any case, the maximum error is 1.33%, what confirms the good behavior of the model.

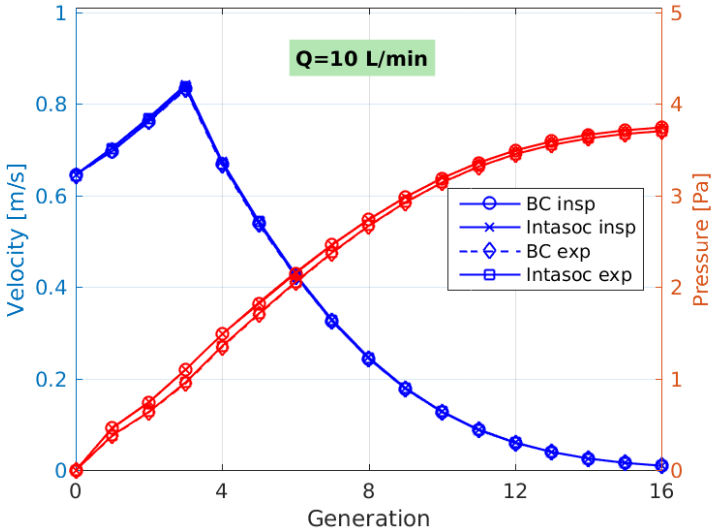


*Figure 4. Velocity and pressure difference on the interior and truncated faces throughout the conductive region during steady state simulations ofinspiration and expiration. Flow rate of 10 L/min*

| | Velocity Error (%) | Pressure Error (%) |
|---|---|---|
| Q = 10 L/min | 1.06 | 0.28 |
| Q = 50 L/min | 0.79 | 0.57 |
| Q = 90 L/min | 0.93 | 1.33 |

*Table 1. Mean relative error for velocity and pressure losses between the truncated face and the intasoc for each of the simulated conditions.*

Another fact of the effective working of the model is the generational variation of velocities. Conclusions of this work agree with those existing in literature (Gemci et al.[12] and Sbirlea-Apiou et al.[27]). At any of the conditions evaluated, it can be observed the velocity increase experienced in the first 3 generations of the airways due to the total cross-sectional area decreases. Then, progressively velocity decreases in the remaining generations as the total cross-sectional area of the lung airway is globally increasing.

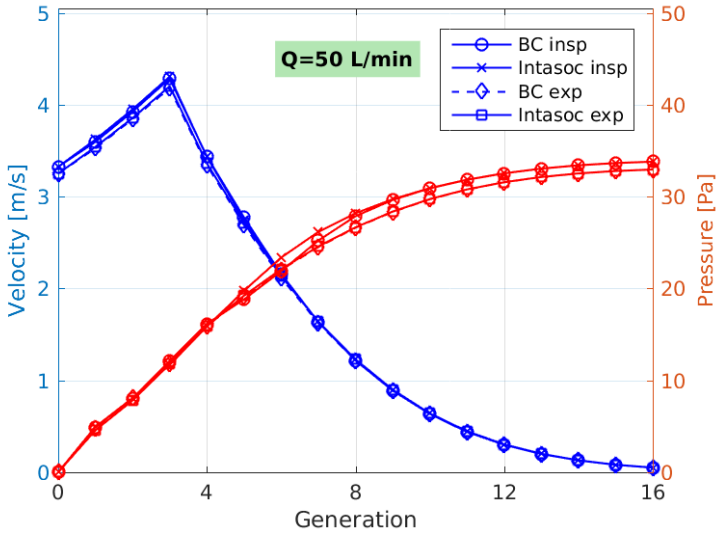


*Figure 5. Velocity and pressure difference on the interior and truncated faces throughout the conductive region during steady state simulations of inspiration and expiration. Flow rate of 50 L/min*

Additionally, it should be highlighted that pressure drop is almost identical for both inspiration and expiration conditions, and also between the truncated face and its symmetrical surface at the conductive branch. This is the normal behavior for a symmetric lung model, where pressure values in each of the daughter airways of a particular bifurcation should be nearly equal. Summarizing, due to the values obtained at the different bc are nearly the same as the objective ones for both inspiration and expiration conditions at each generation while keeping pressure losses are also quite similar, independently of the flow rate considered, confirms the validity of the method employed together with its proper and robust implementation.

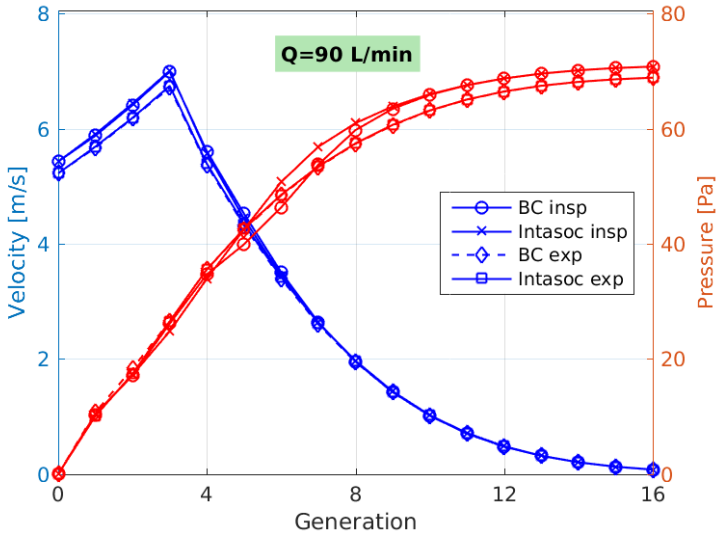


*Figure 6. Velocity and pressure difference on the interior and truncated faces throughout the conductive region during steady state simulations of inspiration and expiration. Flow rate of 90 L/min*

## Weibel's Model Comparison

After checking the accuracy of the boundary condition, a comparison against Weibel's model results is made for a constant flow rate of 50 L/min (a value between sedentary and heavy-activity breathing conditions[24]). Note that in this case both simulations are conducted in the OpenFOAM® platform. In the following figures, contours of static pressure (top) and velocity magnitude (bottom) for the first bifurcation, including some portion of the trachea, are presented in order to compare modelling performance.

Figure 7 depicts CFD results for inspiration process. Regarding velocity contours, a slight departure is observed prior to the bifurcation. Weibel's simulation predicts higher velocities that are coupled with marginally lower pressures. However, the noted differences are totally admissible while the key feature is to reproduce a precisely symmetric flow downstream of the bifurcation with similar flow separation from the wall.

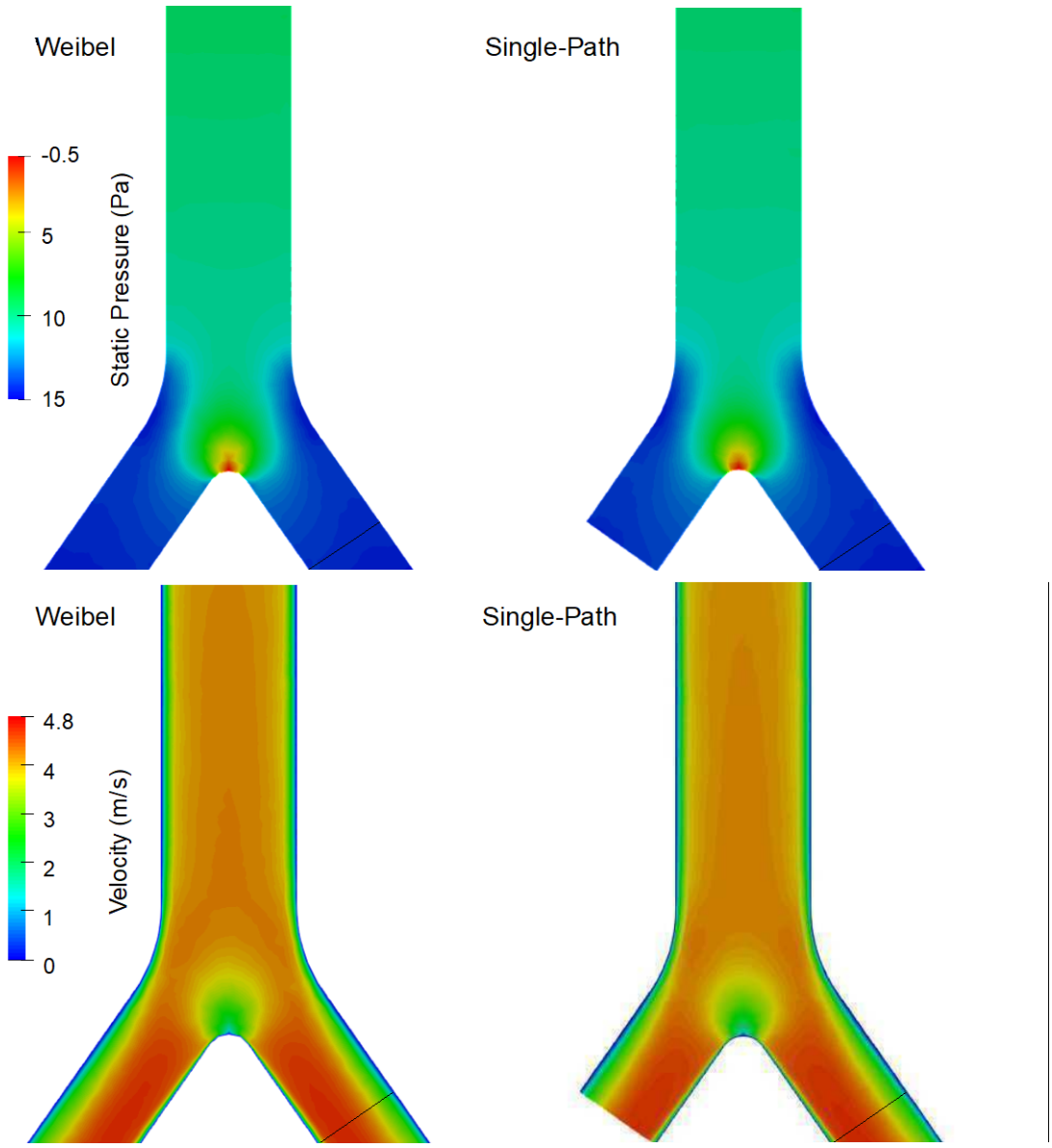


*Figure 7. Contours of the instantaneous static pressure (Pa) (top) and velocity field (m/s) (bottom) on center plane of a bifurcation, generations 0 and 1 during inspiration*

In Figure 8 CFD results for expiration movement are presented. In this case, one can observe again a quite similar behavior between full Weibel's model and the single lung path. Velocity magnitude contours show again the great performance of the boundary condition, which calculates a flow field in great agreement with Weibel's reference. Some minor differences could be noticed at the low velocity region in the middle of the bifurcation (it is slightly wider in the case of Weibel's model), which is also computed in terms of static pressure contours. In any case, the performance of the single lung path model seems remarkable.

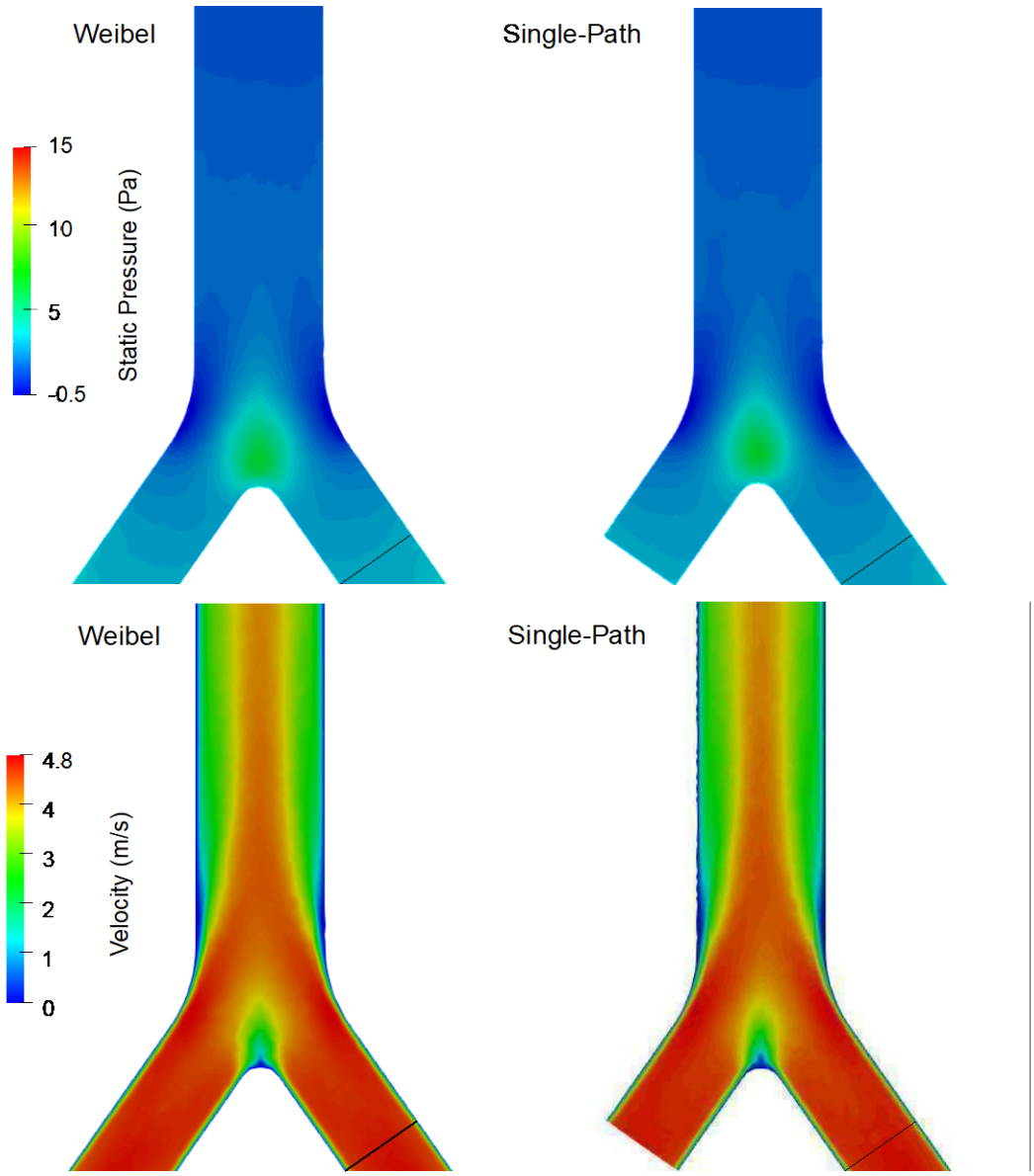


*Figure 8. Contours of the instantaneous static pressure (Pa) (top) and velocity field (m/s) (bottom) on center plane of a bifurcation, generations 0 and 1 during expiration*

Finally, one might question the validity of the method of specifying symmetric velocity. Downstream of generation 2, lung airways are shorter and the flow could have issues to develop completely. Then, at the following bifurcations, the specified velocity would be not correct. To clarify that point, in Figure 9 contours of velocity field at cross-sections are depicted. At the left full Weibel's model generation 0-4 while at the right, single lung path model results are presented. It can be seen the effect in the truncated branches of the centrifugal effect of bifurcation that forces the flow toward one side of the wall. This happens at all truncated branches, though due to the velocity scale used, below generation 4 is not clearly visible. Additionally, a zoom of the contour for generation 4 is shown to compare the results of the single-path against Weibel's model. Velocity contour is quite well predicted, both qualitative and quantitative, which definitely assures the proposed model validity.

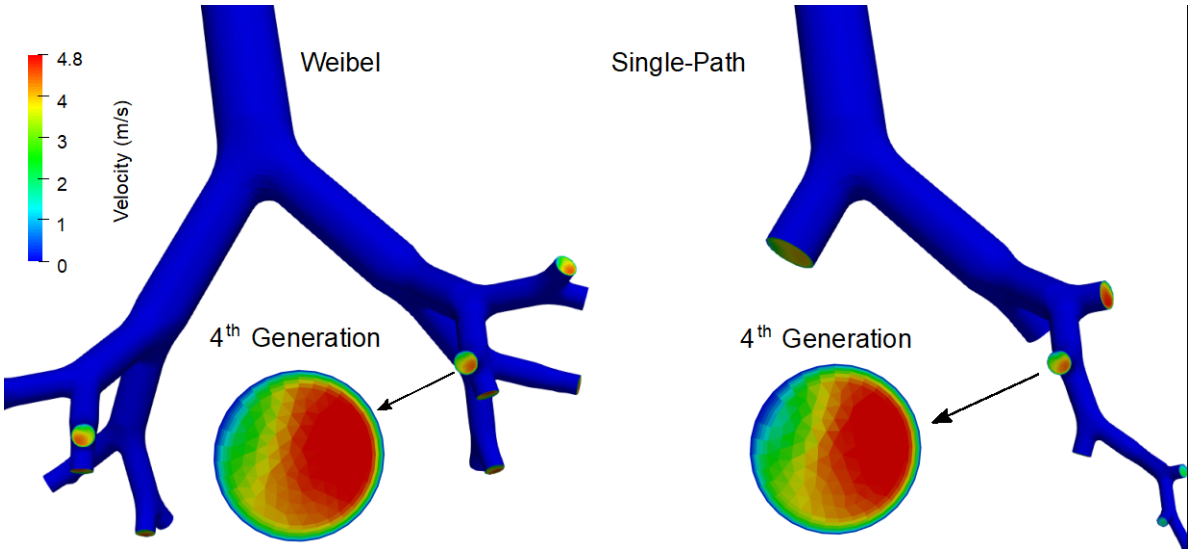


*Figure 9. Contours of velocity field (m/s) at the cross-section on generation 4 during inspiration*

Fluent's Implementation Comparison

Once the boundary condition has been widely validated, a comparison against the Fluent model[9] results is made, again for a constant flow rate of 50 L/min. In the following figures, the same layout as in Figure 7 and 8 is used in order to compare Fluent CFD model results at the left against OpenFOAM® free software ones at the right.

Figure 10 depicts CFD results for inspiration activity. Regarding static pressure contours, although they are quite similar, lower values are obtained with the commercial solver which means that slightly higher velocity ones are computed, due to the total pressure is nearly the same for both simulations. In this kind of simulation, the flow is mainly in the axial direction but it can be detected some differences in regard to the predicted secondary flow. The last one should be greater in the case of OpenFOAM® results due to a greater flow separation with respect to the wall is depicted. However, maybe more important is the completely symmetric flow predicted by the model, while in the case of Fluent velocity field some discrepancies at the inlet of the bifurcation can be seen.

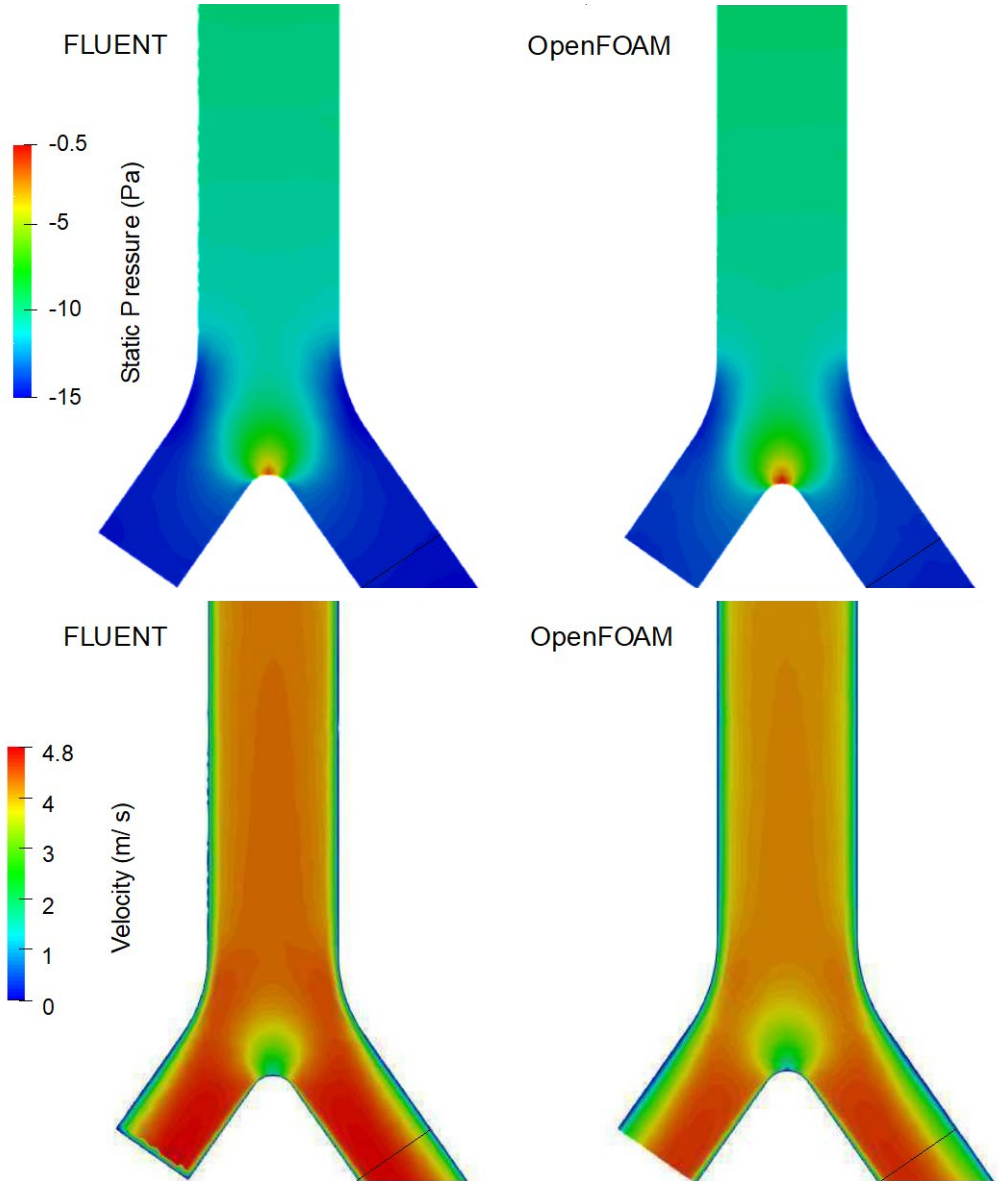


*Figure 10. Contours of the instantaneous static pressure (Pa) (top) and velocity field (m/s) (bottom) on center plane of a bifurcation, generations 0 and 1 during inspiration*

In Figure 11 CFD results for expiration process are presented. In this case, the small differences detected previously are further enhanced, what clearly outlined some Fluent model issues. Velocity magnitude contours show again the great performance of the open-source implementation, which calculates a strictly symmetric flow field as is expected in the case of a symmetric lung model. However, the commercial software produces a no satisfactory solution. It can be seen how the velocity field in the conductive branch is higher than in the truncated one, what progressively decreases the velocity upstream of each bifurcation (after the merging of both path flows) and causes the observed differences regarding static pressure values.

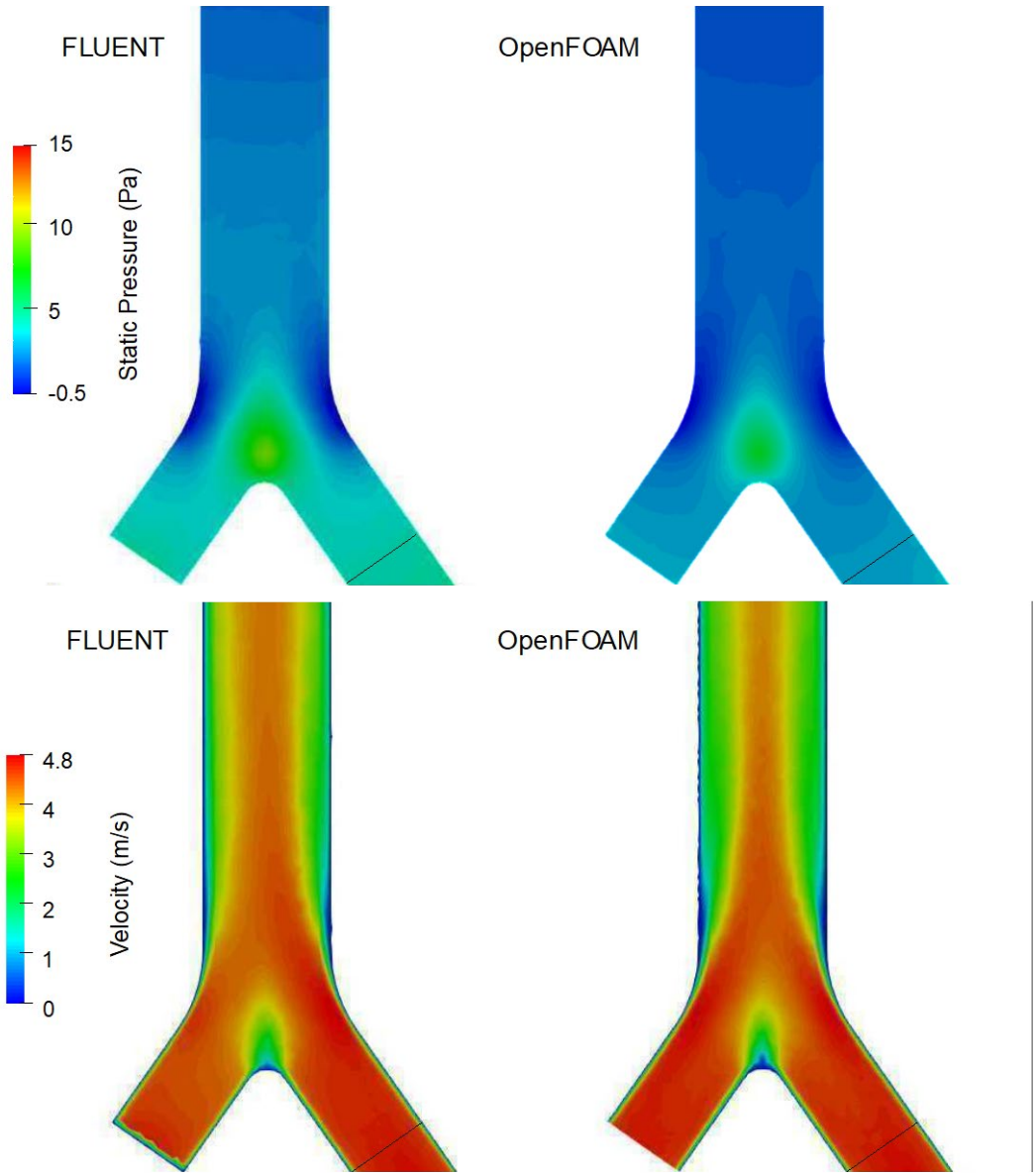


*Figure 11. Contours of the instantaneous static pressure (Pa) (top) and velocity field (m/s) (bottom) on center plane of a bifurcation, generations 0 and 1 during expiration*

**DISCUSSION.**

The forgoing paper has presented an implementation of a special boundary condition for the free commercial software OpenFOAM®, which allows the CFD simulation of a reduced symmetric lung model keeping only one conductive path. The aim of the investigation is to develop this special tool that can be used to complete the geometry obtained with a CT scan and then, a real patient case could be studied with a complete flow including lower generations (see Figure 12). Additionally, this research proves that OpenFOAM® implemented model can perform not only equal as other commercial codes (ANSYS Fluent) but also exceeding its efficiency.

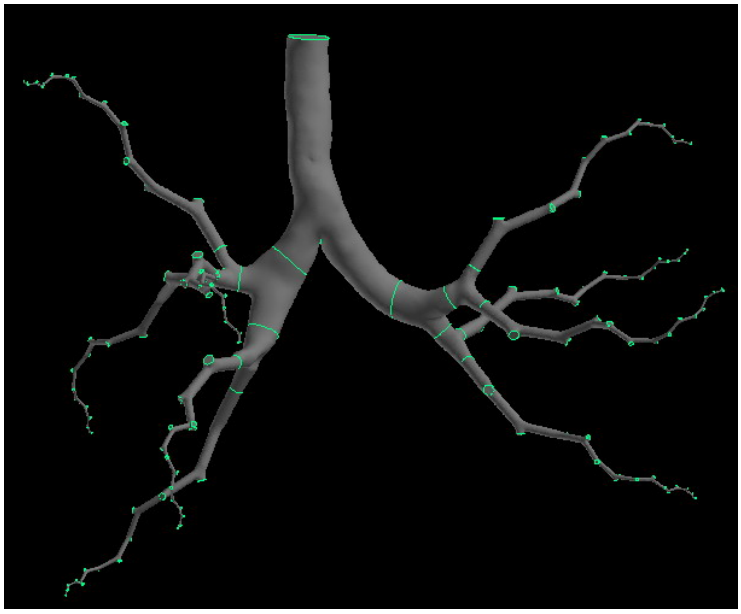

*Figure 12. Geometry constructed coupling a CT scan STL with a symmetric single path ideal lung model*

The construction of the model and the method for applying the physiologically realistic boundary condition follows previous research from Fernández-Tena et al.[9], but with necessary particularities. The computational implementation of the boundary condition on OpenFOAM® is described in detail and afterwards the accuracy of the model is checked and its performance is validated in comparison with a full Weibel's model for 0-4 generation. Finally, modelling results are compare with Fluent implementation of the same boundary condition (implemented through an UDF).

Three different air flow rates are simulated ranging from 10 to 90 L/min, values that represent all the possible normal breathing conditions, including sedentary and heavy-activity breathing. The idea is to evaluate the effectiveness of the implemented boundary condition under these real flow characteristics. In addition, it is proved that the mean error between the quantities at a cross-section of the resolved airway branch and the equivalent boundary location in the truncated branch are limited to admissible values. At the sight of the results, with a maximum error of 1.33%, in the case of the pressure losses, the objective seems to be fulfilled and the boundary condition behaves physiologically realistic including the effect of the truncated airway in the simulations.

Regarding Weibel's model validation, flow accuracy has been effectively demonstrated at medium flow rate condition (50 L/min), for both inspiration and expiration processes, providing a strictly symmetrical flow downstream of a bifurcation at both branches (conductive and truncated airway). Moreover, the centrifugal effect of bifurcation is kept with the model, even if the airway is short with the chance of not having a completely developed flow. This fact ensures the great capabilities and performance of the proposed lung single-path model.

Finally, modelling results of the new model are compared with ANSYS Fluent ones, again for medium flow rate conditions. During inspiration, both software shows a pretty similar behavior providing quite close values in terms of static pressure and velocity magnitude. It can be only noted a slightly different flow path across the bifurcation. Velocity results show

that in case of Fluent code less separation process is predicted and thus, high velocities fill the majority of daughter branches mid-section while in case of OpenFOAM® there is a wider transitional region between the zero velocity value at the walls and the maximum towards the interior of the branch. On the other hand, regarding expiration process major differences can be highlighted. It has been shown that although the velocity is properly copied at the boundary condition, in the case of Fluent solver the developed flow field is not symmetric and a lower velocity value is computed at the truncated branch at the bifurcation. In contrast, OpenFOAM® results exhibit a perfect behavior providing a symmetric flow field upstream of the boundary condition, which proves the better efficiency achieved by the open-source model due to an implementation without any kind of restriction.

Presented results emphasize the invaluable tool that is OpenFOAM® for CFD research and encourage future efforts in the development of the open-source model capabilities applied to the lung flow simulation. The advantage of having access to every level of source program should allow a better implementation/coupling of any kind of new capabilities, e.g. the motion of alveolar sacs with deformable geometry, addition of particle deposition, in order to work properly in conjunction with Navier-Stokes equations. This paper shows that on the basis of the open-source nature of OpenFOAM®, a precise implementation and coupling of the default solver with the in-house functions is achieved and thus, modeling results exceed the performance of other commercial codes which are more limited at implementation capabilities.

## ACKNOWLEDGMENTS.

Authors acknowledge that this work was partially funded by the Spanish Ministry of Economy, Industry and Competitiveness – Instituto de Salud Carlos III under Project “Estudio de la influencia de la geometría de las vías respiratorias en las patologías pulmonares obstructivas (PI17/01639)”, and was supported by Universidad de Oviedo under Project “Desarrollo de nuevo material docente sobre flujos biológicos: simulación de vías áreas humanas. PINN-17-A-061”.

## Compliance with ethical standards

### Conflict of interest

The authors declare that they have no conflict of interest.

## REFERENCES.

1 Adler, K., & Brücker, C. (2007). Dynamic flow in a realistic model of the upper human lung airways. Experiments in Fluids, 43(2-3), 411.

2 ANSYS Fluent Version 6.3.26. ©ANSYS Inc; 2006.

3 ANSYS Gambit Version 2.4.6. ©ANSYS Inc.; 2006.

4 Ball, C. G., Uddin, M., & Pollard, A. (2008). High resolution turbulence modelling of airflow in an idealised human extra-thoracic airway. Computers & Fluids, 37(8), 943-964.

5 Ball, C. G., Uddin, M., & Pollard, A. (2008). Mean flow structures inside the human upper airway. Flow, Turbulence and Combustion, 81(1-2), 155-188.

[6] Beekmans, J. M. (1965). The deposition of aerosol in the respiratory tract: I. Mathematical analysis and comparison with experimental data. Can. J. Physiol. Pharmacol., 43, 157-172.
[7] Davies, C. N. (1961). A formalized anatomy of the human respiratory tract. Inhaled Particles and Vapours, 82-87.
[8] Fernández-Tena, A. (2014). Clinical Applications of Fluid Dynamics Models in Respiratory Disease. PhD Thesis, University of Oviedo, Spain, http://digibuo.uniovi.es/dspace/handle/10651/29057?locale=en.
[9] Fernández-Tena, A., Fernández, J., Álvarez, E., Casan, P., & Walters, D. K. (2017). Design of a numerical model of lung by means of a special boundary condition in the truncated branches. International journal for numerical methods in biomedical engineering, 33(6).
[10] Fernández-Tena, A., Marcos, A. C., Martínez, C., & Keith Walters, D. (2017). A new adaptive time step method for unsteady flow simulations in a human lung. Computer methods in biomechanics and biomedical engineering, 20(8), 915-917.
[11] Findeisen, W. (1935). Über das Absetzenkleiner, in der LuftsuspendierterTeilchen in der menschlichen Lunge bei der Atmung. Pflüger'sArchivfür die gesamtePhysiologie des Menschen und der Tiere, 236(1), 367-379.
[12] Gemci, T., Ponyavin, V., Chen, Y., Chen, H., & Collins, R. (2008). Computational model of airflow in upper 17 generations of human respiratory tract. Journal of Biomechanics, 41(9), 2047-2054.
[13] Grosse S, Schroder W, Klaas M, Klockner A and Roggenkamp J. Time resolved analysis of steady and oscillating flow in the upper human airways. Exp. Fluids. 2007; 42:955–970.
[14] Hegedűs, C. J., Balásházy, I., & Farkas, A. (2004). Detailed mathematical description of the geometry of airway bifurcations. Respiratory physiology & neurobiology, 141(1), 99-114.
[15] Hyatt, R. E., & Wilcon, R. E. (1963). The pressure-flow relationships of the intrathoracic airway in man. The Journal of clinical investigation, 42(1), 29-39.
[16] Kannan R., Chen ZJ, Singh N., et al. (2017). A Quasi-3D wire approach to model pulmonary airflow in human airways. Int J Numer Meth Biomed Engng., 33(7):e2838.
[17] Kannan R., Singh N., Przekwas A. (2018). A compartment-quasi-3D multiscale approach for drug absorption, transport, and retention in the human lungs. Int J Numer Meth Biomed Engng., 34(5):e2955.
[18] Kannan R., Singh N., Przekwas A. (2018). A Quasi-3D compartmental multi-scale approach to detect and quantify diseased regional lung constriction using spirometry data. Int J Numer Meth Biomed Engng., 34(5):e2973.
[19] Kannan R., Guo P., Przekwas A. (2016). Particle transport in the human respiratory tract: formulation of a nodal inverse distance weighted Eulerian-Lagrangian transport and implementation of the Wind-Kessel algorithm for an oral delivery. Int. J. Numer. Meth. Biomed. Engng. 32(6):e2746.
[20] Kannan R., Przekwas A., Singh N., Delvadia R., Tian G., Walenga R., (2017). Pharmaceutical aerosols deposition patterns from a Dry Powder Inhaler: Euler Lagrangian prediction and validation, Medical Engineering & Physics, 42, 35-47.
[21] Kitaoka, H., Takaki, R., & Suki, B. (1999). A three-dimensional model of the human airway tree. Journal of Applied Physiology, 87(6), 2207-2217.

[22] Koullapis, P. G., Hofemeier, P., Sznitman, J., & Kassinos, S. C. (2017). An efficient computational fluid-particle dynamics method to predict deposition in a simplified approximation of the deep lung. European Journal of Pharmaceutical Sciences.
[23] Landahl, H. D. (1950). On the removal of air-borne droplets by the human respiratory tract: I. The lung. The bulletin of mathematical biophysics, 12(1), 43-56.
[24] Nowak, N., Kakade, P. P., & Annapragada, A. V. (2003). Computational fluid dynamics simulation of airflow and aerosol deposition in human lungs. Annals of biomedical engineering, 31(4), 374-390.
[25] OpenFOAM (2017). OpenFOAM Foundation, 2(0).
[26] Sauret, V., Goatman, K. A., Fleming, J. S., & Bailey, A. G. (1999). Semi-automated tabulation of the 3D topology and morphology of branching networks using CT: application to the airway tree. Physics in Medicine & Biology, 44(7), 1625.
[27] Sbirlea-Apiou G, Katz I, Caillibotte G, Martonen T, Yang Y. Deposition mechanics of pharmaceutical particles in human airways. In: Hickey AJ, ed. Inhalation Aerosols. Physical and Biological Basis for Therapy. 2nd ed.New York: Informa Healthcare USA; 2007:1–30.
[28] Schmidt, A., Zidowitz, S., Kriete, A., Denhard, T., Krass, S., & Peitgen, H. O. (2004). A digital reference model of the human bronchial tree. Computerized Medical Imaging and Graphics, 28(4), 203-211.
[29] Tawhai, M. H., & Burrowes, K. S. (2003). Developing integrative computational models of pulmonary structure. The Anatomical Record, 275(1), 207-218.
[30] Theunissen, R., & Riethmuller, M. L. (2007). Particle image velocimetry in lung bifurcation models. In Particle image velocimetry (pp. 73-101). Springer, Berlin, Heidelberg.
[31] Walters, D. K., & Luke, W. H. (2010). A method for three-dimensional Navier–Stokes simulations of large-scale regions of the human lung airway. Journal of Fluids Engineering, 132(5), 051101.
[32] Weibel, E. R. (1963). Geometric and dimensional airway models of conductive, transitory and respiratory zones of the human lung. In Morphometry of the human lung (pp. 136-142). Springer, Berlin, Heidelberg.
[33] Weller, H., Tabor, G., Jasak, H., Fureby, C., 1998. A tensorial approach to computational continuum mechanics using object-oriented techniques. Comput. Phys. 12, 620–631.
[34] Yang, X. L., Liu, Y., & Luo, H. Y. (2006). Respiratory flow in obstructed airways. Journal of biomechanics, 39(15), 2743-2751.
[35] Yang, X. L., Liu, Y., So, R. M. C., & Yang, J. M. (2006). The effect of inlet velocity profile on the bifurcation COPD airway flow. Computers in biology and medicine, 36(2), 181-194.
[36] Zhang, Z., Kleinstreuer, C., & Kim, C. S. (2008). Airflow and nanoparticle deposition in a 16-generation tracheobronchial airway model. Annals of Biomedical Engineering, 36(12), 2095-2110.
[37] Zhang, Z., & Kleinstreuer, C. (2011). Computational analysis of airflow and nanoparticle deposition in a combined nasal–oral–tracheobronchial airway model. Journal of Aerosol Science, 42(3), 174-194.